Functional Characterization of the Ubiquitin Variant Encoded by the Baculovirus *Autographa californica*†

Arthur L. Haas,*,‡ Dean J. Katzung,‡ Patricia M. Reback,‡ and Linda A. Guarino§

Department of Biochemistry, The Medical College of Wisconsin, Milwaukee, Wisconsin 53226, and Department of Entomology, Texas A&M University, College Station, Texas 77843

Received October 19, 1995; Revised Manuscript Received February 20, 1996⊗

ABSTRACT: The marked evolutionary conservation of ubiquitin is assumed to arise from constraints imposed by folding, stability, and interaction of the polypeptide with various components of the ATP,ubiquitin-dependent degradative pathway. The present studies characterize the most divergent (75% identity) of the species-specific ubiquitin isoforms encoded as a late gene product of the baculovirus *Autographa californica* [Guarino, L. A. (1990) *Proc. Natl. Acad. Sci. U.S.A. 87*, 409−413]. Viral ubiquitin supports 40% of the rate of ATP-dependent degradation exhibited by eukaryotic ubiquitin. Inhibition of proteolysis correlated with a lower steady-state concentration of ubiquitin-conjugated degradative intermediates. Rate studies revealed that viral ubiquitin exerts its effect at the step of isopeptide ligase-catalyzed (E3) ubiquitin conjugation since viral and eukaryotic polypeptides are identical in their abilities to support ATP-coupled activation by E1 and transthiolation to E2 carrier proteins. Other studies demonstrated viral ubiquitin severely attenuated the rate of K48-linked multiubiquitin chain formation in E3-independent conjugation catalyzed by recombinant yeast CDC34 or rabbit reticulocyte $E2_{32K}$ but not chain elongation of alternate linkages formed by yeast RAD6 or human $E2_{EPF}$. The latter observations suggest nonconserved positions on viral ubiquitin constitute recognition signals for K48-linked chain formation. Sequence comparison of species-specific ubiquitin isoforms indicates that nonconserved positions localized to a defined region on the polypeptide surface distinct from the basic face required for E1 binding. These results suggest this novel ubiquitin isoform may function in baculoviral replication to block destruction of a short-lived protein(s) by the host degradative pathway, targeted through either E2-catalyzed K48-linked multiubiquitin chain formation or general E3-mediated conjugation.

Ubiquitin is a highly conserved 8.6 kDa protein distributed universally among eukaryotes (Goldstein et al., 1975; Schlesinger et al., 1975). The polypeptide was thought to be absent from prokaryotes; however, detection of ubiquitin in the eubacterium *Anabaena variabilis* (Durner & Boger, 1995) suggests this protein and its allied enzymes arose during the evolutionary transition from true prokaryotes to eukaryotes. Early evidence suggested an extracellular site of action as a circulating peptide hormone since ubiquitin exhibited the ability to stimulate lymphocyte differentiation through an adenylate cyclase-mediated pathway (Goldstein et al., 1975; Schlesinger et al., 1975, 1978). However, the principal biological roles of ubiquitin are now recognized to be manifested intracellularly through its covalent ligation to various target proteins, reviewed most recently by Hochstrasser (1995). Ubiquitin conjugation targets the attached protein for degradation by the 26S proteasome, with subsequent recycling of ubiquitin by specific cleavage of the carboxyl-terminal isopeptide bond. Formation on the target protein of a multiubiquitin chain in which the carboxyl terminus of each polypeptide is linked to K48 of the preceding ubiquitin commits the protein to degradation through binding to subunit 5 of the 26S proteasome regulatory complex (Chau et al., 1989; Deveraux et al., 1994).

The mechanism for conjugating the carboxyl-terminal glycine of ubiquitin to lysyl ϵ-amino groups of target protein substrates is understood in some detail (Haas & Bright, 1988; Pickart, 1988), eqs 1−3.[1] Ubiquitin activating enzyme (E_{SH})

$$E_{SH} + ATP + Ub \rightleftarrows E_{S\sim Ub} + AMP + PP_i \quad (1)$$

$$E_{S\sim Ub} + E2_{SH} \rightleftarrows E_{SH} + E2_{S\sim Ub} \quad (2)$$

$$E2_{S\sim Ub} + \text{protein}-NH_2 \overset{E3}{\rightleftarrows} E2_{SH} + \text{protein}-NH-Ub \quad (3)$$

catalyzes the ATP-coupled activation of the carboxyl terminus of ubiquitin to form a ternary complex composed of 1 equiv each of tightly bound ($K_d \leq 10^{-14}$ M) ubiquitin adenylate and covalently bound ubiquitin thiolester (Haas & Rose, 1982; Haas et al., 1982), with only the latter intermediate being represented in eq 1. The thiolester intermediate is catalytically transferred to any of a family of ubiquitin carrier protein isozymes ($E2_{SH}$) via a transthiolation reaction (eq 2). Formation of an isopeptide bond between ubiquitin and the target protein is catalyzed by one of several ubiquitin:protein isopeptide ligase isozymes, termed E3 (Hershko et al., 1983; Lee et al., 1986; Reiss et

† This work was supported in part by U.S. Public Health Service Grants GM34009 (to A.L.H.) and GM44055 (to L.A.G.).

* Author to whom correspondence should be addressed.
‡ The Medical College of Wisconsin.
§ Texas A&M University.

⊗ Abstract published in *Advance ACS Abstracts,* April 15, 1996.

[1] Abbreviations: BSA, bovine serum albumin; E1, ubiquitin activating enzyme; E2, ubiquitin carrier protein; E3, protein:ubiquitin isopeptide ligase; rcmBSA, reduced carboxymethylated BSA; Ub, ubiquitin [e, eukaryotic (referenced to human sequence); v, baculoviral; rm, reductively methylated].

S0006-2960(95)02498-6 CCC: $12.00

al., 1989; Bartel et al., 1990; Huibregtse et al., 1993). Mammalian isopeptide ligase(s) form(s) K48-linked multiubiquitin homopolymer chains in the presence of the major cognate E2 isozyme, $E2_{14K}$.[2] Other E2 isozymes, notably the rabbit $E2_{32K}$ and yeast CDC34 isoforms, are catalytically competent to support facile multiubiquitin homopolymer formation specifically at K48 in the absence of E3, suggesting the potential for unique protein specificities independent of the normal pathway for protein targeting (Haas et al., 1988, 1990).

The marked conservation in the sequence of ubiquitin is assumed to arise by constraints imposed by its folding and interaction with various enzymes involved in ubiquitin-mediated degradation (Jentsch et al., 1990). Moreover, sequence conservation implies that mutations are either lethal or subject to rapid negative selection. Across the plant and animal kingdoms amino acid substitutions are tolerated at only a limited number of positions, all of which represent conservative replacements and have no functional consequence where previously tested (Vierstra et al., 1985; Wilkinson et al., 1986). Therefore, it was surprising when one of us (L.A.G.) identified a significantly divergent ubiquitin mutant within an open reading frame of the genome for the baculovirus *Autographa californica* (Guarino, 1990). The inferred sequence of viral ubiquitin is 75% homologous to eukaryotic ubiquitin, with most of the substitutions occurring within and flanking the single 3.5 turn α helix identified in the 1.8 Å crystal structure of the latter (Vijay-Kumar et al., 1987). Although the presence of ubiquitin within the baculovirus genome likely arose by recombination, its retention suggests the protein confers some selective advantage.[3] Various observations indicate that baculoviral ubiquitin is coexpressed with viral coat proteins as a late gene product in the replicative cycle of the virus (Guarino, 1990; Guarino et al., 1995). In addition, viral ubiquitin may be involved in the formation of viral particles since deletion of the viral ubiquitin gene results in a 5−10-fold reduction in the yield of infectious virus (Reilly & Guarino, 1996).

The present studies were initiated to test the ability of baculoviral ubiquitin to support ATP-dependent conjugation and degradation. The results provide insight into the potential role(s) of viral ubiquitin in the replicative cycle of baculovirus, the constraints on structure−function imposed upon eukaryotic ubiquitin through evolution, and evidence for the spatial segregation of protein−protein contact sites on the surface of the polypeptide.

EXPERIMENTAL PROCEDURES

Materials. Eukaryotic ubiquitin (bovine) was purchased from Sigma and used without further purification. Aliquots of pure eukaryotic and viral ubiquitins were radioiodinated by the chloramine T method (Haas & Rose, 1982). Quantitative reductive methylation of eUb and vUb by formaldehyde and $NaCNBH_4$ was as described previously (Haas et al., 1988). Recombinant eUbK48R was that used in earlier studies (Haas et al., 1991). Preparation of reduced carboxymethylated ^{125}I-BSA (Pentex) was modified (Haas & Rose, 1981) from that of Evans and Wilkinson (1985). Tetrasodium [^{32}P]pyrophosphate, carrier-free Na^{125}I, and [2,8-^{3}H]ATP were purchased from Amersham Radiochemicals. Rabbit reticulocyte fraction II free of endogenous eukaryotic ubiquitin was prepared by DEAE-cellulose chromatography and stored at −80 °C in small aliquots (Haas & Rose, 1981). The rabbit reticulocyte E1 and the indicated E2 isozymes were those described previously (Haas et al., 1988). Crude E3 fractions were prepared from fraction II by 30% saturated ammonium sulfate fractionation (Haas et al., 1988). Bovine thymus core histone H2A was the generous gift of Vaughn Jackson (Medical College of Wisconsin). Recombinant mature vUb in which a STOP codon was inserted prior to the Y77 "capping" codon present in the viral precursor vUbY77 (Guarino, 1990) was expressed and purified as previously described (Guarino et al., 1995).

Protein Degradation Assays. Initial rates of ^{125}I-rcmBSA degradation were measured by formation of TCA-soluble radioactivity in 60 min incubations containing 50 mM Tris-HCl (pH 7.5), 2 mM ATP, 10 mM $MgCl_2$, 10 mM creatine phosphate, 1 IU/mL creatine phosphokinase, 1 mM DTT, and the indicated concentrations of ubiquitin, ^{125}I-rcmBSA, and reticulocyte fraction II protein (Haas & Rose, 1981). When ubiquitin was omitted from the assays, rates of degradation in the absence or presence of ATP were comparable and generally represented only 5−10% of the velocity in the presence of saturating eUb.

Enzyme Assays. Ubiquitin activating enzyme was assayed by the initial rate of ATP−$^{32}PP_i$ exchange in the presence of 1 mM AMP to kinetically isolate step 1 of the reaction and to avoid potential effects due to subsequent E1−ubiquitin thiolester formation (Haas & Rose, 1982). The net forward rate of E1 was measured as the stoichiometric hydrolysis of [γ-^{32}P]ATP hydrolysis in the presence of yeast inorganic pyrophosphatase by coupling the reaction to recombinant yeast RAD6-catalyzed histone conjugation in the presence of saturating ATP, ubiquitin, and histone (Haas et al., 1988). Initial rates of radiolabeled ubiquitin conjugation were determined after resolution of free ^{125}I-ubiquitin from its conjugates by SDS−PAGE followed by quantitation of the latter by γ counting of the resulting dried gel (Haas & Rose, 1981; Haas et al., 1988).

RESULTS

Viral Ubiquitin Fails To Fully Support ATP-Dependent Proteolysis. Figure 1A compares the concentration dependence of eUb versus vUb on the initial rate of ATP-dependent ^{125}I-rcmBSA degradation by rabbit reticulocyte fraction II, which contains all components required for the proteolytic pathway except ubiquitin. The dependence of eUb concentration on the initial rate of degradation plateaus sharply above 5 μM polypeptide and is nonhyperbolic, based on the nonlinearity of a corresponding reciprocal plot (not shown). The unusual kinetic behavior suggests a change in rate-limiting step from E1-dependent activation at low concentrations of eUb to a subsequent step within the pathway at higher concentrations. This interpretation and the low apparent $K_{1/2}$ for eUb in Figure 1A are consistent with the reported K_d of 0.58 μM for E1 binding of ubiquitin (Haas & Rose, 1982). A similar concentration dependence is observed with vUb; however, the limiting rate for vUb is only 35%

[2] A. L. Haas and P. M. Reback, unpublished observations.

[3] A ubiquitin sequence is also present within the CP1 genome of cytopathogenic bovine viral diarrhea virus (Meyeres et al., 1991); however, in this case the presence of ubiquitin probably functions to introduce an internal processing site into the gene, resulting in enhanced pathogenicity.

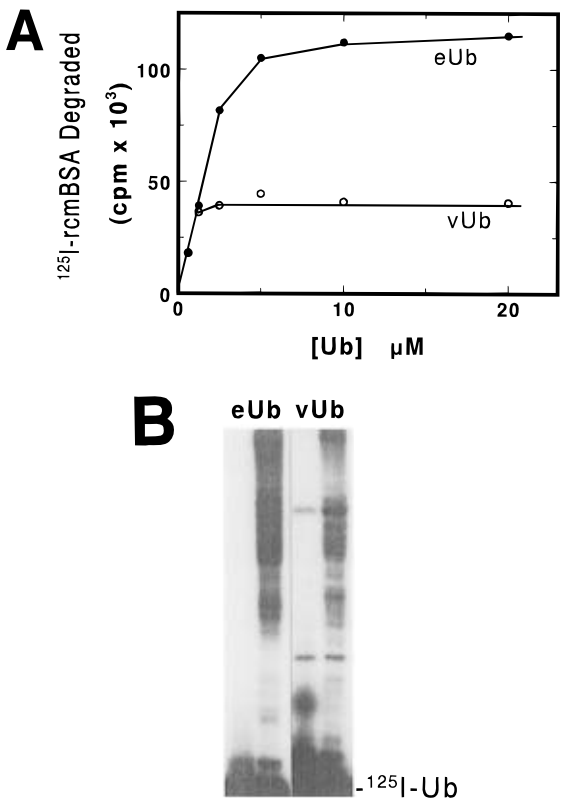

FIGURE 1: Ubiquitin dependence for supporting ATP-dependent proteolysis. (A) The initial rate of ^{125}I-rcmBSA degradation to TCA-soluble radioactivity was determined as described in Experimental Procedures. Incubations of 60 min contained 240 μg of fraction II protein, 1.9 μM ^{125}I-rcmBSA (26 000 cpm/pmol), and the indicated concentrations of either eUb (closed circles) or vUbY77 (open circles). (B) The steady-state distribution of conjugates was determined autoradiographically after SDS−PAGE resolution. Reactions identical to those for the 10 μM points of panel A contained either ^{125}I-eUb (7200 cpm/pmol, left panel) or ^{125}I-vUb (1300 cpm/pmol, right panel) and were incubated for 60 min before quenching with SDS sample buffer and boiling for 2 min. Samples were resolved on 10% SDS−PAGE gels, dried, and autoradiographed. Exposures were adjusted to correct for the difference in specific activities between the ubiquitin variants. For the control lanes (left lane of each panel) radiolabeled ubiquitin was added after quenching with SDS sample buffer.

of that observed for eUb (Figure 1A). The inability of vUb to fully support ATP-dependent degradation was highly reproducibile in replicate experiments with different preparations of vUb or fraction II for which the apparent V_{max} for viral ubiquitin varied from 35% to 45% relative to that found with eUb (not shown).

The steady-state distribution of conjugates formed between the ubiquitin variants and endogenous fraction II proteins was determined under the same conditions as for the 10 μM concentration point of Figure 1A using either ^{125}I-eUb or ^{125}I-vUb and unlabeled rcmBSA (Figure 1B). The pattern of conjugates formed with ^{125}I-vUb was qualitatively similar to that found with ^{125}I-eUb (Figure 1B), although the absolute amount of ^{125}I-vUb conjugates was significantly attenuated as indicated by the lower autoradiographic intensity in the upper portion of the corresponding lanes after normalizing exposure times for differences in the specific radioactivities of the two polypeptides. Steady-state levels of conjugates formed with the radioiodinated ubiquitin variants were quantitated by cutting the test lanes from the dried gel and determining bound radioactivity by γ counting (Haas & Rose, 1981). These values were corrected for small amounts of radioactivity present in the respective control lanes incubated in the absence of ATP. The steady-state amount of conjugates formed to ^{125}I-vUb was 39% of that observed with ^{125}I-eUb, in good agreement with the difference in apparent V_{max} for supporting ATP-dependent degradation in Figure 1A. Correspondence between the steady-state levels of conjugates and the relative abilities of the ubiquitin variants to support degradation was consistently observed among different preparations of vUb and fraction II (not shown).

The Effect of vUb in Supporting Degradation Results from a Lower Rate of Conjugation. The results of Figure 1 indicate the inability of vUb to fully support ATP-dependent degradation resulted from a proportionately lower concentration of conjugate intermediates. Since the steady-state concentration of these adducts depends on the relative magnitudes of the opposing steps of conjugate formation, conjugate disassembly, and conjugate degradation [reviewed in Haas (1988)], the lower fractional level of conjugation found with vUb compared to eUb could potentially result from a slower rate of conjugate formation, an increased rate of conjugate disassembly, an increased rate of conjugation degradation, or any combination of the three effects.

We discounted an enhanced rate of vUb conjugate degradation since this alternative was inconsistent with the initial observation that vUb supported only 35% of the rate of degradation found with eUb (Figure 1A). If the effect of vUb occurred at a step after initial fragmentation of the ^{125}I-rcmBSA−vUb conjugates, then it remained possible that any enhanced degradation of vUb adducts would result in the accumulation of large, TCA-insoluble peptides that would remain undetected by the proteolytic assay. Two observations ruled out the latter alternative. No accumulation of ^{125}I-rcmBSA peptides was observed in the presence of vUb compared to eUb by SDS−PAGE (not shown), and the qualitative size distribution of ^{125}I-vUb conjugates did not show a shift to lower molecular weights compared to those formed to ^{125}I-eUb (Figure 1B).

Differences in steady-state levels of eUb versus vUb conjugates also did not result from enhanced disassembly of the viral ubiquitin conjugate pool. Rates of conjugate disassembly were compared between ^{125}I-vUb and ^{125}I-eUb by first allowing conjugates to reach steady state as in Figure 1B and then rapidly depleting the reactions of ATP by adjusting the incubation to 10 IU/mL yeast hexokinase and 20 mM 2-deoxyglucose, after which aliquots were taken at various times to quantitate levels of conjugates by γ counting following SDS−PAGE resolution as in Figure 1B. Conjugates to ^{125}I-vUb and ^{125}I-eUb both displayed the biphasic kinetics for disassembly observed previously (Haas & Rose, 1981; Chin et al., 1982) (Figure 2). Graphical analysis appropriate to such biphasic kinetics yielded comparable half-lives for the initial rapid first-order disassembly phase that directly correlates with rates of degradation (Haas & Rose, 1981) (inset to Figure 2). The limiting slow rate of conjugate disassembly was comparable between eUb (0.15 min^{-1}) and vUb (0.11 min^{-1}). In contrast, vUb yielded a slightly smaller pool of rapidly disassembled conjugates compared to eUb, as shown by the difference in intercept values when the slow linear phase was extrapolated to zero time (Figure 2). These observations preclude an effect on the bulk rate of vUb conjugate disassmebly, compared to that of eUb adducts, as a mechanism to account for the lower steady-state concentra-

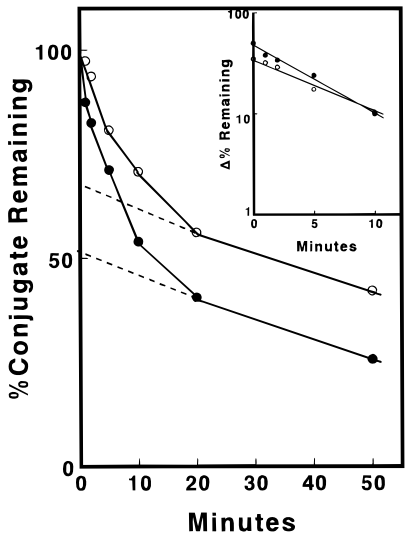

FIGURE 2: Disassembly kinetics for eUb versus vUb. Steady-state incubations such as in Figure 1B contained either ^{125}I-eUb (solid circles) or ^{125}I-vUb (open circles). At zero time the incubations were adjusted to 20 mM 2-deoxyglucose and 10 IU/mL yeast hexokinase, after which samples were removed at the indicated times and quenched into SDS sample buffer. Conjugates were quantitated as described in Experimental Procedures. Inset: first-order plot of the initial rapid phase of conjugate disassembly graphically corrected for the slower limiting rate of conjugate loss.

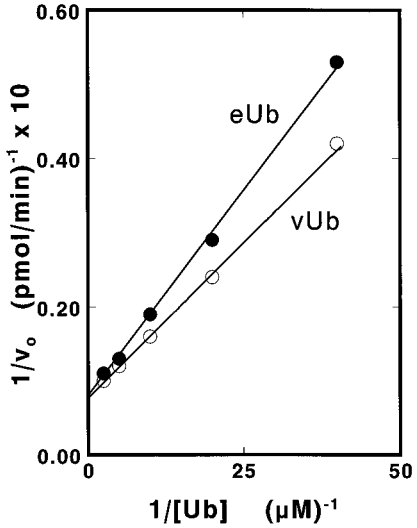

FIGURE 3: Comparison of eUb and vUb in E1-catalyzed ATP−PP_i exchange. Initial rates of reticulocyte E1-catalyzed ATP−$^{32}PP_i$ exchange were measured in the presence of 10 nM activating enzyme and either eUb (solid circles) or vUb (open circles).

tion of the former from Figure 1B; however, the results do not rule out an effect of vUb on specific isopeptidases that do not significantly contribute kinetically to overall conjugate disassembly under the conditions of the degradation assays in Figure 1A.

Initial rates for approach to steady state of ^{125}I-vUb and ^{125}I-eUb conjugation were measured under the conditions of Figure 1B (not shown). The initial rate of ^{125}I-vUb conjugation (5.8 pmol/min) was 36% of the rate for eUb (16.3 pmol/min), again in good agreement with the observed differences in apparent V_{max} for ^{125}I-rcmBSA degradation (Figure 1A) and steady-state levels of conjugates (Figure 1B). The data therefore indicated the inability of vUb to fully support ATP, ubiquitin-dependent degradation resulted for some step of the conjugation pathway, leading to a lower rate of adduct formation. Since the mechanism of ubiquitin−protein conjugation is fairly well understood and most of the components of this pathway have been isolated to apparent homogeneity, it was possible to kinetically isolate each step in order to determine the point at which vUb affected the rate of ligation.

Viral and Eukaryotic Ubiquitins Are Kinetically Equivalent in Their Carboxyl-Terminal Activation. Recombinant vUb was compared to eUb in its ability to support E1-catalyzed ATP−$^{32}PP_i$ exchange, the first step in the pathway for both E3-dependent and E3-independent ubiquitin conjugation (Haas & Rose, 1982; Hershko et al., 1983; Haas & Bright, 1988). Figure 3 shows reciprocal plots for the initial rates of $^{32}PP_i$ exchange catalyzed by homogeneous activating enzyme prepared by a combination of covalent affinity and FPLC chromatography (Haas & Bright, 1988). Both eUb and vUb exhibited identical V_{max} values of 133 pmol/min, corresponding to a k_{cat} of 4.4 s^{-1}, in good agreement with the value of 5.6 s^{-1} determined previously (Haas & Rose, 1982). Values for $K_{1/2}$ of 0.15 μM and 0.11 μM for eUb and vUb, respectively, were within the limit of discrimination for this assay. At higher concentrations both eUb and vUb exhibited substrate inhibition of the exchange reaction, a characteristic feature of ordered substrate addition for which ATP is the leading and ubiquitin the trailing substrate (Haas & Rose, 1982). The rate studies of Figure 3 were conducted in the presence of 1 mM AMP to kinetically isolate step 1 of the E1 reaction, involving formation of tightly bound ubiquitin adenylate, from the subsequent step of ubiquitin transfer to the E1 thiolester site (Haas & Rose, 1982). Results similar to those of Figure 3 were obtained in the absence of AMP, indicating that vUb also had no effect on the overall formation of E1 ternary complex containing both noncovalently bound ubiquitin adenylate and ubiquitin thiolester (Haas & Rose, 1982). This conclusion was confirmed by the ability of ^{125}I-vUb to form a stoichiometric thiolester with E1 (not shown).

We have recently shown the kinetics of E1-catalyzed ATP−PP_i exchange are a poor indicator of potential effects that mutation of ubiquitin may have on the affinity of the activating enzyme for the polypeptide (Burch & Haas, 1994). Therefore, the intrinsic K_d for vUb binding to E1 was measured by quantitating the equilibrium formation of vUb [^{3}H]adenylate under conditions of varying ATP and vUb (Haas & Rose, 1982) (not shown). The dependence of vUb [^{3}H]adenylate formation on [ATP] and [vUb] conformed to the mathematical model previously established for eUb and yielded a K_d for vUb of 1.28 μM, in reasonable agreement with the value of 0.58 μM reported for eUb (Haas & Rose, 1982). These studies also provided an estimate for the equilibrium constant for the catalytic step of bound ubiquitin adenylate formation, K_3', of 0.10 for vUb, which was in good agreement with the value of 0.16 for eUb (Haas & Rose, 1982). Therefore, the substitutions present on vUb do not significantly affect either the binding or subsequent adenylate formation steps with the activating enzyme.

The rate studies of Figure 3 do not address the potential effect of vUb on the net forward rate of ubiquitin activation catalyzed by E1 since exchange kinetics are necessarily measured under equilibrium conditions. To address this question, the net forward rate of E1 was determined by coupling this step to the E3-independent conjugation of histone H2A catalyzed by the yeast recombinant E2 isozyme

Table 1: Viral Ubiquitin Does Not Affect the Net Forward Velocity of E1[a]

	[γ-^{32}P]ATP hydrolyzed (pmol)	H2A conjugated (pmol)
experiment 1 (eUb)		
+E1	0.3	
+E1, RAD6	4.0	
+E1, RAD6, H2A	21.1	17.1
experiment 2 (vUb)		
+E1, RAD6	3.8	
+E1, RAD6, H2A	20.1	16.3

[a] Incubations of 20 min were conducted as described in Experimental Procedures under E1 limiting conditions using 1 nM E1, 20 nM RAD6, 8.5 μM histone H2A, and 5 μM eUb or vUb.

RAD6 (Haas et al., 1988, 1990). Initial rates of H2A conjugation were measured by quantitating the stoichiometric hydrolysis of [γ-^{32}P]ATP in the presence of yeast inorganic pyrophosphatase (Chen et al., 1991) (Table 1). Assays were conducted under conditions of rate-limiting E1, determined by the linearity of rate with respect to [E1]. In Table 1 the amount of [γ-^{32}P]ATP hydrolyzed in the presence of E1 alone or in combination with RAD6 represents that required for the burst loading of the E1 ternary complex (2 ATP/equiv of E1), formation of RAD6 thiolester (1 ATP/equiv of RAD6), and the subsequent slow transfer of ubiquitin thiolester intermediates to DTT present in the incubations (Haas et al., 1982). A significantly greater rate of [γ-^{32}P]-ATP hydrolysis is observed on addition of H2A as a substrate for conjugation (Table 1). When the ATP hydrolyzed in the presence of H2A was corrected for that required for loading of E1 and RAD6, the resulting net rate of H2A conjugation was comparable between eUb and vUb (Table 1).

Other control experiments (not shown) demonstrated that (1) the net [γ-^{32}P]ATP hydrolyzed in the presence of H2A was stoichiometric with the addition of ^{125}I-eUb to the histone by RAD6, determined by quantitation of γ counts following SDS−PAGE resolution (Haas et al., 1988); (2) the increase in [γ-^{32}P]ATP hydrolysis in the presence of H2A represented an increase in the limiting rate of ATP hydrolysis without an effect on the burst loading of either E1 or RAD6; and (3) no increase in the rate of [γ-^{32}P]ATP hydrolysis was observed in the presence of H2A if either E1 or RAD6 was omitted from the incubations, ruling out the presence of contaminating ATPase activity in the apparently homogeneous H2A preparation. The results of Figure 3, Table 1, and the equilibrium measurements of ubiquitin adenylate formation indicate that E1 is kinetically incapable of distinguishing between eUb and vUb in either its equilibrium or net forward rate of ubiquitin activation. Therefore, the lower initial rate of vUb conjugation leading to the attenuated steady-state concentration of these adducts observed in Figure 1B does not result from a kinetic defect in vUb activation.

Viral and Eukaryotic Ubiquitins Differ in Their Abilities To Support E3-Dependent Conjugation. The yeast E2 isozyme RAD6 catalyzes an E3-independent conjugation reaction yielding ubiquitin conjugates specifically degraded by the 26S multicatalytic protease complex (Haas et al., 1990), supports E3-dependent conjugation with rabbit reticulocyte E3 (Haas et al., 1991), and mediates E3-dependent degradation through an N-end rule recognition pathway in yeast (Sung et al., 1991). Cell-free complementation experiments in rabbit reticulocyte extracts show that $E2_{14K}$, the mammalian RAD6 homolog (Schneider et al., 1990; Wing et al., 1992), is the major cognate isozyme for E3-dependent degradation (Pickart & Rose, 1985; Haas et al., 1991; Baboshina & Haas, 1996).[4] Accordingly, we were interested in comparing viral and eukaryotic ubiquitins in $E2_{14K}$-dependent conjugation.

Table 2: Viral Ubiquitin Does Not Affect $E2_{14K}$-Dependent Conjugation by Isopeptide Ligase[a]

	initial velocity (pmol/min)	
	eUb	vUb
0.1 nM E1, 25 nM $E2_{14K}$	0.33 (0.34)	0.35 (0.37)
0.2 nM E1, 25 nM $E2_{14K}$	0.43 (0.44)	0.43 (0.47)
2.0 nM E1, 25 nM $E2_{14K}$	0.84 (0.86)	0.83 (0.90)
2.0 nM E1, 50 nM $E2_{14K}$	1.12 (1.15)	1.13 (1.23)

[a] Incubations were for 20 min at 37 °C as described in Experimental Procedures for incubations of 50 μL total volume containing the indicated concentrations of E1 and recombinant $E2_{14K}$ and 150 μg of crude E3 protein. Numbers in parentheses are predicted initial rates based on the assay conditions and kinetic parameters reported previously (Haas et al., 1988).

Table 2 summarizes representative rate data comparing eUb and vUb in supporting E3-dependent conjugation under either E1- or $E2_{14K}$-limiting conditions. The complementation studies of Table 2 were conducted with a crude preparation of rabbit reticulocyte E3 free of contaminating E1 or E2 isozymes (Haas & Bright, 1988) to which homogeneous rabbit E1 and $E2_{14K}$ were added. Endogenous proteins present in the crude E3 fraction served as substrates for conjugation. Under conditions of rate-limiting [E1] (0.1 or 0.2 nM) and 25 nM $E2_{14K}$, rates of E3-dependent conjugation were identical between eUb and vUb. The proportionality of the initial conjugation rates with respect to [E1] confirmed the activation step to be rate limiting. The dependence of rate on [E1] compared favorably with that predicted from the reported apparent $K_{1/2}$ of 0.1 nM for binding of $E2_{14K}$ to E1 ternary complex (Haas & Bright, 1988). These results support the conclusion from Table 1 that E1 does not distinguish between eUb and vUb in the net forward reaction of ubiquitin activation and further shows this effect to be independent of the E2 isozyme. Likewise, the observed initial ligation rates under $E2_{14K}$-limiting conditions (25 or 50 nM) and saturating E1 (2 nM) were identical between eUb and vUb. Again, the proportionality of the initial rates to [$E2_{14K}$] confirmed the E2 step to be rate limiting for the incubation conditions. The dependence of rate on [$E2_{14K}$] under the latter experimental conditions agreed with that expected from the kinetically determined apparent K_m of 25 nM for $E2_{14K}$−ubiquitin thiolester binding to E3 (Haas et al., 1988) (predicted values shown in parentheses for Table 2).

The results of Table 2 indicate that eUb and vUb are functionally indistinguishable when the E1 and E2 steps are kinetically isolated within the pathway of E3-dependent conjugation. At $E2_{14K}$ concentrations above those used in Table 2, the dependence of carrier protein concentration on the observed rate of E3-mediated conjugation increased hyberbolically in the presence of 5 μM eUb, an effect

[4] Rabbit reticulocyte $E2_{14K}$ exists in two functionally equivalent isoforms designated $E2_{14Ka}$ and $E2_{14Kb}$ (Haas & Bright, 1988). All present studies were conducted with the more abundant rabbit "b" isoform.

Table 3: Comparison of eUb and vUb in Supporting E3-Dependent Conjugation[a]

	[E2] (nM)	v_0 (pmol/min) eUb	vUb	% v_{eUb}
$E2_{14K}$	200	1.25	0.55	44
$E2_{20K}$	56	0.27	0.09	35
$E2_{32K}$	88	0.21	0.04	20
CDC34	32	0.20	0.06	32
RAD6	540	0.51	0.20	39

[a] Incubations were conducted as described in Table 2 under E3 limiting conditions and the indicated concentrations of homogeneous E2 isozyme. Concentrations of the E2 isozymes were chosen to be 8-fold above their apparent K_m for binding of their respective ubiquitin thiolester to E3 (Haas et al., 1988, 1991). The extreme right column lists the initial velocity observed with vUb as a percent of that observed for eUb.

previously exploited to determine the K_m for $E2_{14K}$−ubiquitin thiolester binding to E3 (Haas et al., 1991). In contrast, when the latter rate study was repeated with vUb, the rate of conjugation plateaued sharply, suggesting a shift in rate-limiting step for E3-dependent ligation (not shown). This new rate-limiting step in the presence of vUb and high [$E2_{14K}$] must reside in the step catalyzed by E3 since any further increase in [E1] had no effect on the observed rate (not shown). Table 3 demonstrates that the initial rate of ^{125}I-vUb ligation is 44% of that observed for ^{125}I-eUb, under conditions of rate-limiting [E3] achieved at saturating [$E2_{14K}$] equal to 8 times the experimentally determined K_m for binding of the latter thiolester to the isopeptide ligase (Haas et al., 1991).

The rate data with $E2_{14K}$ indicate that the lower rate of conjugation and the resulting inability of vUb to fully support ATP, ubiquitin-dependent degradation (Figure 1) reside in the E3-catalyzed step of ligation. Parallel rate studies with other reticulocyte and recombinant yeast E2 isozymes previously shown to support E3-dependent ligation (Haas et al., 1988, 1991) demonstrate that the kinetic defect present with vUb is a general feature of E3-dependent conjugation (Table 3). Thus, all five isozymes listed in Table 3 exhibit initial rates of ^{125}I-vUb conjugation under E3-limiting conditions that range from 20% to 44% of that observed with eUb.

Viral Ubiquitin Does Not Block Multiubiquitin-Dependent Degradation. The lower rate of vUb ligation in rate-limiting E3-dependent conjugation does not result from an inability of this variant to support K48-linked multiubiquitination. This was shown by comparing the efficacy of different ubiquitins to support net ATP,ubiquitin-dependent degradation of ^{125}I-rcmBSA (Table 4). Degradation assays similar to those of Figure 1A were conducted with reticulocyte fraction II and various ubiquitins. The greatest rate of degradation was observed with wild-type eUb. When reductively methylated eUb (rmeUb) was substituted for wild-type polypeptide, the initial rate of ^{125}I-rcmBSA degradation was reduced to 19% of that observed with native eUb (Table 4). Reduction in the rate of degradation results from the inability of rmeUb to support multiubiquitination at the derivatized lysines. Most of the multiubiquitin-dependent degradation must proceed through formation of isopeptide bonds at K48 of ubiquitin since UbK48R, in which K48 has been substituted for arginine by site-directed mutagenesis (Chau et al., 1989; Gregori et al., 1990), shows a similar decline in supporting

Table 4: Viral Ubiquitin Supports Multiubiquitin-Dependent Degradation[a]

	net ATP/Ub-dependent rate (cpm)	%
eUb	54 100	100
rmeUb	10 500	19
UbK48R	12 700	24
vUb	22 600	42
rmvUb	1 200	2

[a] Initial rates for degradation of saturating ^{125}I-rcmBSA were measured as described in Experimental Procedures in the presence of 10 μM ubiquitin variant in 60 min assays. Rates of degradation are averages of triplicate determinations and have been corrected for basal activity in the absence of added ubiquitin, representing ~10% of the net ATP/ubiquitin-dependent velocity.

degradation. The slightly higher rate of degradation with UbK48R compared to rmeUb was consistently observed and suggests some degradation proceeds through multiubiquitination at site(s) other than K48 (Table 4), as shown by independent experiments with E2 isozymes capable of E3-independent multiubiquitination (Haas et al., 1990) and $E2_{EPF}$/E3-dependent K11-linked multiubiquitin proteolysis (Baboshina & Haas, 1996). The rate of vUb-dependent degradation under saturating conditions was 42% of that observed with eUb, as found in Figure 1A. However, when rmvUb was substituted for native vUb, the rate of degradation was only 2% of that found with eUb. The decrease in rate of degradation with rmvUb compared to vUb suggests that vUb is catalytically competent qualitatively to support multiubiquitination since rmvUb is otherwise kinetically identical to vUb in the E1-catalyzed activation step (not shown); however, the results do not rule out the possibility that vUb affects the rate of chain elongation and hence the steady-state level of total vUb conjugates (Figure 1A). That the rate of degradation supported by rmvUb (2%) is less than that observed for rmeUb (19%) is consistent with conclusions above that the rate-limiting step of ubiquitin-mediated proteolysis is E3 dependent under the assay conditions employed.

E3-Independent K48 Multiubiquitination Is Blocked by vUb. The data of Table 4 indicate that sequence differences between eUb and vUb do not block the ability of the latter to support E3-dependent K48 multiubiquitination. However, during the course of these studies we found that vUb does significantly affect the rate of K48 multiubiquitination by the two E2 isozymes previously shown specifically to catalyze formation of this linkage through an E3-independent mechanism (Haas et al., 1990, 1991).

Recombinant yeast CDC34 exhibits marked kinetic specificity for forming K48-linked multiubiquitin homopolymers to itself in the absence of isopeptide ligase (Haas et al., 1991; Banerjee et al., 1993; Ptak et al., 1994). In the autoradiogram of Figure 4 a total of nine ubiquitins become linked to CDC34 when saturating ^{125}I-eUb is included in the incubation. The apparent absence of a band corresponding to CDC34−Ub_4 results from a kinetic effect under steady-state conditions for which the subsequent addition of a fifth ubiquitin to this species is faster than its rate of formation.[5] The modest steady-state level of the monoubiquitin intermediate is consistent with previous observations that this

[5] D. J. Katzung and A. L. Haas, in preparation.

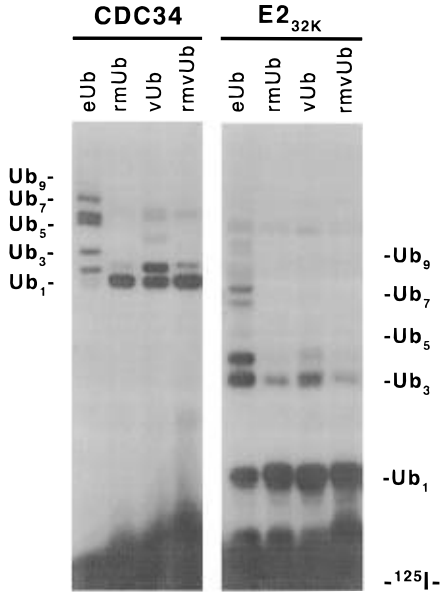

FIGURE 4: vUb does not support E3-independent K48-linked multiubiquitination. The E3-independent autoubiquitination of recombinant CDC34 (left panel) and the $E2_{32K}$-catalyzed conjugation of histone H2A (right panel) were examined in incubations of 50 μL final volume containing 50 mM Tris-HCl (pH 7.5), 2 mM ATP, 10 mM $MgCl_2$, 10 mM creatine phosphate, 1 IU/mL creatine phosphokinase, 5 μM indicated radioiodinated ubiquitin variant, 38 nM E1, 16 μM H2A ($E2_{32K}$ lanes only), and 84 nM CDC34 or 20 nM $E2_{32K}$. Reactions were quenched after 20 min at 37 °C by addition of SDS sample buffer, after which samples were resolved by 12% SDS−PAGE (Haas et al., 1988). Sample volumes were normalized to correct for variation in the specific activities of the ubiquitin variants. Positions of ^{125}I-ubiquitin and conjugate bands of the indicated linkage number are shown to the sides.

reaction is highly processive (Haas et al., 1991).[6] In contrast, this monoubiquitin adduct accumulates in the presence of ^{125}I-rmeUb, which is incapable of multiubiquitination (Figure 4). Except for a small amount of ubiquitination at a second site on CDC34, the absence of higher adducts with the reductively methylated ubiquitin indicates that these latter species must exist in multiubiquitin linkage (Haas et al., 1991). Multiubiquitination catalyzed by CDC34 is exclusively through isopeptide bond formation to K48 since conjugation patterns identical to those with ^{125}I-rmeUb are observed with ^{125}I-UbK48R (Haas et al., 1991). In a parallel incubation, the conjugate pattern with ^{125}I-vUb resembled that observed with ^{125}I-rmeUb, with the exception that substantially more of the diubiquitin adduct is formed. However, most of the di-vUb adduct must represent a truncated CDC34−vUb_2 homopolymer since this band is greatly diminished in the presence of ^{125}I-rmvUb (Figure 4). On longer exposure of Figure 4, a pattern of multiubiquitin bands could be observed with ^{125}I-vUb that was not present with ^{125}I-rmvUb (not shown), indicating a rate effect for vUb multiubiquitination.

We have previously shown that rabbit reticulocyte $E2_{32K}$ is also capable of specific, highly processive K48 multiubiquitination using core histones as model substrates (Haas et al., 1988, 1990, 1991). Under the incubation conditions of Figure 4 homopolymer chains extend to H2A−Ub_9 since no larger adducts than that of a trace amount of a diubiquitin species are observed in the presence of ^{125}I-rmeUb. As with CDC34, earlier work has shown that the multiubiquitin linkage formed by $E2_{32K}$ is through K48 of ubiquitin by comparison to patterns formed with ^{125}I-UbK48R (Haas et al., 1990, 1991). Low steady-state accumulation of bands corresponding to $E2_{32K}$−Ub_2 and $E2_{32K}$−Ub_5 arise from a kinetic effect analogous to that observed with the tetraubiquitin band of CDC34.[5] Viral ubiquitin is unable to support multiubiquitination beyond that of a low level of a diubiquitin adduct, most of which must exist as a truncated homopolymer rather than to a second site on the histone substrate since this latter band is greatly diminished when ^{125}I-rmvUb is substituted (Figure 4). Longer exposure of Figure 4 revealed a pattern of H2A-linked multiubiquitin bands with ^{125}I-vUb not present in the corresponding ^{125}I-rmvUb lane, indicating a rate effect of vUb on chain elongation by $E2_{32K}$ (not shown).

The results of Figure 4 indicate that the inability of vUb to support K48 multiubiquitination is independent of either the E2 isozyme or substrate and is therefore highly specific for such multiubiquitination. This apparent effect is not a consequence of differences in E1-catalyzed activation since none of the ubiquitin variants used in Figure 4 are kinetically distinguishable by ATP−PP_i exchange (Haas et al., 1991),[2] nor is the effect due to differences in net E2-dependent conjugation since the autoradiographic intensities of the monoubiquitin adducts are similar, in agreement with data presented above showing that the E2 step is not affected by substituting vUb for eUb. However, the effect is specific for K48 multiubiquitination since no difference in conjugation pattern for homopolymer formation is observed with either recombinant yeast RAD6 or recombinant human $E2_{EPF}$, both of which catalyze formation of ubiquitin chains at site(s) distinct from K48 (Haas et al., 1991; Liu et al., 1992; Baboshina & Haas, 1996) (not shown).[5]

DISCUSSION

Marked conservation in the amino acid sequence of ubiquitin among eukaryotes has been assumed to arise by selective pressures over the entire surface of the protein in response to interactions with multiple enzymes within the ATP,ubiquitin-dependent degradative pathway. However, with the exception of early limited studies using site-directed mutagenesis (Ecker et al., 1987) and chemical modification (Duerksen-Hughes et al., 1987) and more recent work exploiting systematic mutagenesis (Burch & Haas, 1994; Baboshina & Haas, 1996),[5] this hypothesis has not been rigorously examined. The present studies with the viral ubiquitin homolog have allowed us kinetically to isolate each step in the conjugation reaction and provide the first direct evidence for segregation of functional surfaces on the polypeptide.

Comparison of the amino acid sequences of vUb and eUb relative to the secondary and tertiary structures of the latter reveals that the majority of the amino acid changes defining alteration in side-chain polarity lie on the surface of the molecule. Interestingly, all of the nonconservative changes present on vUb localize to the surface of ubiquitin occupied by or near the 3.5 turn α helix (Figure 5A). Except for the R54K substitution, none of the nonconserved residues lie on the basic face of ubiquitin defined by the four arginine

[6] Within this context processivity is defined as the enhanced ability of a ubiquitin conjugate to serve as a substrate for further multiubiquitination without consideration of whether the responsible conjugating enzyme remains bound to the adduct during the reaction.

residues, three of which (R42, R54, and R72) participate in binding of the polypeptide to E1 from chemical modification studies (Duerksen-Hughes et al., 1987) and more recently confirmed by site-directed mutagenesis (Burch & Haas, 1994). Spatial clustering of substitutions on vUb outside of the initial E1−ubiquitin contact surface is consistent with the inability of the ubiquitin activating enzyme to distinguish between vUb and eUb in direct measurements of the intrinsic K_d for ubiquitin binding (see text), support of ATP−PP_i exchange (Figure 3), or in overall conjugation (Tables 1−3). The data also indicate substitutions on vUb do not markedly affect the folding or packing of the molecule and the α-helical face of the polypeptide is not required for binding to E1. That the conserved R54K substitution on vUb has no effect on binding while UbR54L binds with significantly lower affinity (Burch & Haas, 1994) suggests interaction between E1 and ubiquitin at this position must involve a Coulombic effect. This conclusion has been directly confirmed with the point mutant UbR54K, which exhibits a K_d for binding to E1 identical to that of wild-type polypeptide (Baboshina & Haas, 1996).

In contrast, by kinetically isolating each step in the conjugation reaction, it has been possible to demonstrate that the E3-catalyzed step of ligation does discriminate between eUb and vUb, accounting for the inability of vUb to fully support both wild-type rates of conjugation and net ATP, ubiquitin-dependent protein degradation (Figure 1). This conclusion is supported by the good agreement between inhibition of the overall degradation and the initial rate of conjugate formation. The defect observed with vUb does not arise by inability of the viral protein to support K48 multiubiquitination since substitution of rmvUb, which is incapable of forming extended ubiquitin chains, shows a further reduction in the initial rate of ^{125}I-rcmBSA degradation (Table 4). Moreover, the results of Table 4 indicate the effect on degradation is specific for E3-catalyzed multiubiquitination and is independent of the E2 isoform employed (Table 3).

Attenuation in the rate of E3-catalyzed conjugation by vUb can be satisfied by either of three models. If residues mutated on vUb normally interact with the catalytic core domain within the $E2_{S\sim eUb}$ complex to anchor ubiquitin to the carrier protein, then the presumably greater conformational flexibility of the $E2_{S\sim vUb}$ thiolester may not be catalytically competent to support E3-dependent conjugation at wild-type rates. That similar effects of vUb are observed with all isozymes of E2 tested (Table 3) requires these putative E2−ubiquitin interactions to be conserved within

```
 1 MQIFVKTLTG KTITLEVEPS DTIENVKAKI QDKEGIPPDQ QRLIFAGKQL EDGRTLSDYN IQKESTLHLV LRLRGG
 2 ----I----- ----A-T--A E-VADL-Q-- A----V-V-- ---------- --SK-MA--- --------M- ------
 3 ---------- --------S- ---D------ ---------- ---------- ------A--- ---------- ------
 4 ---------- --------A- ---------- ---------- ---------- ---------- ---------- ------
 5 ---------- --------S- ---------- ---------- ---------- ---------- ---------- ------
 6 ---------- ------D--- ---------- ---------- ---------- ---------- ---------- ------
 7 ---------- ------D-Q- ---D---T-- ---------- ---------- ------A--- ---------- ------
 8 ---------- --------S- ---D---S-- ---------- ---------- ---------- ---------- ------
 9 ---------- ---------- ---D------ ---------- ---------- ------A--- ---------- ------
10 ---------- ---------- -S-------- ---------- ---------- ---------- ---------- ------
11 ---------- --------G- -N-------- ---------- ---------- ---------- ---------- ------
12 ---------- ---A----A- ---------- ---------- ---------- -E----A--- ---------- ------
13 ---------- ---------- ---------- ---------- ---------- G--------- ---------- ------
14 ---------- --------S- ---D---Q-- ---------- ---------- ---------- ---------- ------
15 ---------- --------S- ---------- ---------- ---------- ------A--- ---------- ------
16 ---------- ---------A
17 ---------- ---------N -S-DAI---- -E-------- ---------- -E-K------ ---------- ------
 1 MQIFVKTLTG KTITLEVEPS DTIENVKAKI QDKEGIPPDQ QRLIFAGKQL EDGRTLSDYN IQKESTLHLV LRLRGG
```

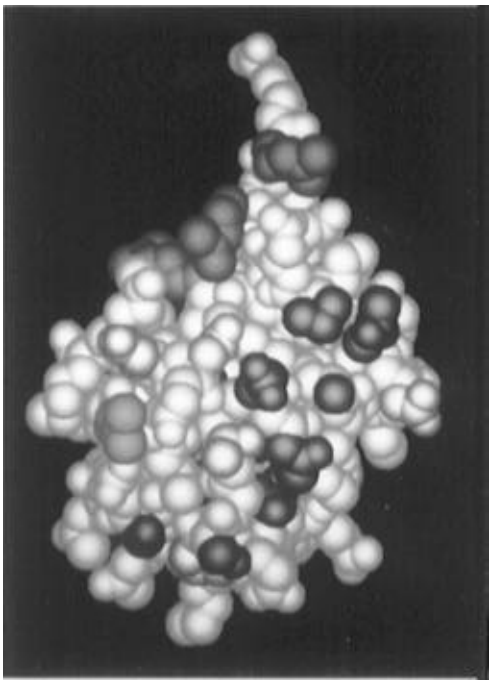

FIGURE 5: Sequence comparison of ubiquitin isoforms. Panel A (top): Sequence comparison among the species-specific ubiquitin isoforms for which conserved positions are indicated by −: 1, mammalian; 2, *A. californica*; 3, *Arabidopsis thaliana*, soybean, wheat, oat; 4, *Caenorhabditis elegans*; 5, inky cap fungus; 6, *Plasmodium faciparum*; 7, *Euplotes eurystomus*; 8, *Saccharomyces cerevisiae*; 9, barley; 10, sea urchin; 11, *Dictyostelium discoideum*; 12, *Trypanosoma brucei*; 13, fall army worm; 14, *Neurospora crassa*; 15, *Chlamydomonas rheinhardii*; 16, *Thermoplasma acidophilum*; 17, *Entamoeba histolytica*. Panel B (bottom left): Nonconserved positions listed in panel A for vUb (red) and other species-specific variants (gold) are highlighted on the 1.8 Å crystal structure of human ubiquitin (Vijay-Kumar et al., 1987) except for position 54 of vUb, which is light blue. The four arginine residues comprising the basic contact face for binding to E1 (Burch & Haas, 1994) are shown in shades of blue for orientation. The carboxyl terminus of the polypeptide is at the top of the figure.

the family. More recent studies with the vUb-derived point mutant UbN25D support this interpretation in affecting E3-independent conjugation among a variety of E2 isozymes.[5] Alternatively, the effect of vUb on conjugation could arise by disrupting key interactions within the $E3{\cdot}E2_{S\sim Ub}$ Michaelis complex if both ubiquitin and E2 moieties directly interact with ligase and the mutated residue(s) of vUb are normally required for binding. Decreased affinity of rabbit E3α for the nonfunctional product analog $E2_{14K}C88A$ compared to the corresponding substrate $E2_{S\sim Ub}$ suggests ubiquitin directly interacts with the ligase, consistent with the latter interpretation.[7] Finally, vUb may attenuate the rate of E3-catalyzed multiubiquitin chain elongation similar to that of E3-independent conjugation (Figure 4). Work is currently in progress to distinguish among these alternate models.

Although vUb supports K48 multiubiquitination within the E3-dependent conjugation pathway (Table 4), the viral protein severely attenuates E3-independent chain formation for those E2 isozymes catalyzing this reaction (Figure 4). Results of Figure 4 are not a consequence of K48-linked chain destabilization since none of the vUb mutations participate in packing interactions between ubiquitin subunits within this structure (Cook et al., 1994). Inability of vUb to support K48 multiubiquitin chain elongation suggests that some or all of the mutations contained within the polypeptide represent recognition sites required for chain elongation. Since vUb attenuates chain elongation at the $-Ub_2$ stage for CDC34 and the $-Ub_3$ stage for $E2_{32K}$, fidelity in forming K48 isopeptide bonds beyond these points probably requires $E2_{S\sim Ub}$ to bind across multiple subunits within the multiubiquitin chain. Recognition of a three-dimensional constellation of sites on the growing chain as a requirement for elongation affords considerable accuracy for the process. That vUb affects chain elongation by yeast CDC34 and rabbit $E2_{32K}$ requires these putative interactions to be conserved between the two isozymes. Such an interpretation requires a K_m effect for recognition of vUb chains, consistent with the significantly reduced but not blocked elongation observed on prolonged exposure of the autoradiogram of Figure 4.

Figure 5A compares sequences among eUb, vUb, and the species-specific isoforms of ubiquitin reported to date. Nearly all of the species-specific substitutions cluster within two regions of the ubiquitin sequence, with most appearing within the α-helical segment. When the nonconserved positions are superimposed on the 1.8 Å crystal structure of ubiquitin (Vijay-Kumar et al., 1987), they localize within a defined region adjacent to the basic face defined by the four arginine residues that comprise the contact surface with E1 (Burch & Haas, 1994) (Figure 5B). The vUb mutations also cluster within the same region defined by the species-specific variants. Such segregation on the surface of the polypeptide accounts for the inability of E1 to distinguish between mammalian ubiquitin and those from yeast (Wilkinson et al., 1986), plant (Vierstra et al., 1985), and vUb (this study). Since the ubiquitin-dependent degradation pathway is required for cell viability, the cluster of residues highlighted in Figure 5B must not be required for the overall function of the pathway but probably are required for specialized roles not shared among all organisms. Therefore, if a particular specialized role(s) is absent from a given species, ubiquitin residues participating in this process(es) would not be constrained by natural selection unless required for other globally conserved functions. This interpretation is consistent with differential expression of E2 isozymes within eukaryotes [reviewed in Hochstrasser (1995)] and function-specific segregation of regions or residues on the surface of the polypeptide.

An early recombination event must have originally incorporated the host ubiquitin gene within the baculoviral genome. Subsequent retention of the ubiquitin coding sequence indicates the polypeptide provides some selective advantage; however, liberated from functional constraints of the host, the gene diverged in sequence to its present form. That sequence divergence has been restricted to the cluster defined by the species-specific isoforms (Figure 5B) requires the selective advantage provided by vUb must involve its ligation through the host conjugation pathway during viral replication. Since vUb is expressed as a late gene during expression of viral coat proteins (Guarino, 1990), it is tempting to speculate that vUb protects viral structural proteins against destruction by the general ATP,ubiquitin-dependent degradative pathway of the host. Such an interpretation requires vUb to accumulate to sufficient levels to effectively compete with host eUb for entry into the conjugation pathway during E1-catalyzed activation. Such a scenario is plausible given the characteristic block in host cell protein synthesis accompanying viral infection and the short half-life of ubiquitin [discussed in Haas (1988)]. Model studies with rabbit reticulocyte fraction II show mole ratios of vUb/eUb up to 20:1 inhibit degradation of ^{125}I-rcmBSA by only 5%.[5] This level of protection might provide sufficient selective advantage to allow reduced yield of virus particles and is consistent with the attenuation in viral replication produced by mutant virus (Reilly & Guarino, 1996). Alternatively, vUb may block a specific E2-mediated targeting function within the host by acting as a chain terminator of K48-linked multiubiquitin chain elongation, resulting in stabilization of a constitutively short-lived protein(s) required for efficient viral replication. This hypothesis is consistent with the greater sensitivity of E3-independent multiubiquitination (Figure 4) to vUb compared to E3-dependent ligation (Figure 1).

The present studies extend our structure−function analysis of ubiquitin and identify evolutionary constraints on the molecule imposed by its interaction with enzymes of the ubiquitin-dependent degradative pathway. Future work will no doubt identify other examples, such as the E2 isozyme encoded by African swine flue virus (Hingamp et al., 1992), in which nature has coopted components of this pathway to serve novel functions or to block existing roles for ubiquitin ligation.

[7] T. Siepmann and A. L. Haas, in preparation.

REFERENCES

Baboshina, O. V., & Haas, A. L. (1996) *J. Biol. Chem. 271*, 2823−2831.

Banerjee, A., Gregori, L., Xu, Y., & Chau, V. (1993) *J. Biol. Chem. 268*, 5668−5675.

Bartel, B., Wunning, I., & Varshavsky, A. (1990) *Embo J. 9*, 3179−3189.

Burch, T. J., & Haas, A. L. (1994) *Biochemistry 33*, 7300−7308.

Chau, V., Tobias, J. W., Bachmair, A., Marriott, D., Ecker, D. J., Gonda, D. K., & Varshavsky, A. (1989) *Science 243*, 1576−1583.

Chen, Z. J., Niles, E. G., & Pickart, C. M. (1991) *J. Biol. Chem. 266*, 15698−15704.

Chin, D. T., Kuehl, L., & Rechsteiner, M. (1982) *Proc. Natl. Acad. Sci. U.S.A. 79*, 5857−5861.
Cook, W. J., Jeffrey, L. C., Kasperek, E., & Pickart, C. M. (1994) *J. Mol. Biol. 236*, 601−609.
Deveraux, Q., Ustrell, V., Pickart, C., & Rechsteiner, M. (1994) *J. Biol. Chem. 269*, 7059−7061.
Duerksen-Hughes, P. J., Xu, X. X., & Wilkinson, K. D. (1987) *Biochemistry 26*, 6980−6987.
Durner, J., & Boger, P. (1995) *J. Biol. Chem. 270*, 3720−3725.
Ecker, D. J., Butt, T. R., Marsh, J., Sternberg, E. J., Margolis, N., Monia, B. P., Jonnalagadda, S., Khan, M. I., Weber, P. L., Mueller, L., et al. (1987) *J. Biol. Chem. 262*, 14213−14221.
Evans, A. C., Jr., & Wilkinson, K. D. (1985) *Biochemistry 24*, 2915−2923.
Goldstein, G., Scheid, M., Hammerling, U., Boyse, E. A., Schlesinger, D. H., & Niall, H. D. (1975) *Proc. Natl. Acad. Sci. U.S.A. 72*, 11−15.
Gregori, L., Poosch, M. S., Cousins, G., & Chau, V. (1990) *J. Biol. Chem. 265*, 8354−8357.
Guarino, L. A. (1990) *Proc. Natl. Acad. Sci. U.S.A. 87*, 409−413.
Guarino, L. A., Smith, G., & Dong, W. (1995) *Cell 80*, 301−309.
Haas, A. L. (1988) in *Ubiquitin* (Rechsteiner, M., Ed.) pp 173−206, Plenum Press, New York, NY.
Haas, A. L., & Rose, I. A. (1981) *Proc. Natl. Acad. Sci. U.S.A. 78*, 6845−6848.
Haas, A. L., & Rose, I. A. (1982) *J. Biol. Chem. 257*, 10329−10337.
Haas, A. L., & Bright, P. M. (1988) *J. Biol. Chem. 263*, 13258−13267.
Haas, A. L., Warms, J. V., Hershko, A., & Rose, I. A. (1982) *J. Biol. Chem. 257*, 2543−2548.
Haas, A. L., Bright, P. M., & Jackson, V. E. (1988) *J. Biol. Chem. 263*, 13268−13275.
Haas, A., Reback, P. M., Pratt, G., & Rechsteiner, M. (1990) *J. Biol. Chem. 265*, 21664−21669.
Haas, A. L., Reback, P. B., & Chau, V. (1991) *J. Biol. Chem. 266*, 5104−5112.
Hershko, A., Heller, H., Elias, S., & Ciechanover, A. (1983) *J. Biol. Chem. 258*, 8206−8214.
Hingamp, P. M., Arnold, J. E., Mayer, R. J., & Dixon, L. K. (1992) *Embo J. 11*, 361−366.
Hochstrasser, M. (1995) *Curr. Opin. Cell Biol. 7*, 215−223.
Huibregtse, J. M., Scheffner, M., & Howley, P. M. (1993) *Mol. Cell. Biol. 13*, 775−784.
Jentsch, S., Seufert, W., Sommer, T., & Reins, H. A. (1990) *Trends Biochem. Sci. 15*, 195−198.
Lee, P. L., Midelfort, C. F., Murakami, K., & Hatcher, V. B. (1986) *Biochemistry 25*, 3134−3138.
Liu, Z., Diaz, L. A., Haas, A. L., & Giudice, G. J. (1992) *J. Biol. Chem. 267*, 15829−15835.
Meyers, G., Tautz, N., Dubovi, E. J., & Thiel, H. J. (1991) *Virology 180*, 602−616.
Pickart, C. M. (1988) in *Ubiquitin* (Rechsteiner, M., Ed.) pp 77−99, Plenum Press, New York, NY.
Pickart, C. M., & Rose, I. A. (1985) *J. Biol. Chem. 260*, 1573−1581.
Ptak, C., Prendergast, J. A., Hodgins, R., Kay, C. M., Chau, V., & Ellison, M. J. (1994) *J. Biol. Chem. 269*, 26539−26545.
Reilly, L. M., & Guarino, L. A. (1996) *Virology* (in press).
Reiss, Y., Heller, H., & Hershko, A. (1989) *J. Biol. Chem. 264*, 10378−10383.
Schlesinger, D. H., Goldstein, G., & Niall, H. D. (1975) *Biochemistry 14*, 2214−2218.
Schlesinger, D. H., Goldstein, G., Scheid, M. P., & Bitensky, M. (1978) *Experientia 34*, 703−704.
Schenider, R., Eckerskorn, C., Lottspeich, F., & Schweiger, M. (1990) *EMBO J. 9*, 1431−1435.
Sung, P., Berleth, E., Pickart, C., Prakash, S., & Prakash, L. (1991) *Embo J. 10*, 2187−2193.
Vierstra, R. D., Langan, S. M., & Haas, A. L. (1985) *J. Biol. Chem. 260*, 12015−12021.
Vijay-Kumar, S., Bugg, C. E., & Cook, W. J. (1987) *J. Mol. Biol. 194*, 531−544.
Wilkinson, K. D., Cox, M. J., O'Connor, L. B., & Shapira, R. (1986) *Biochemistry 25*, 4999−5004.
Wing, S. S., Dumas, F., & Banville, D. (1992) *J. Biol. Chem. 267*, 6495−6501.

BI9524981